JOURNAL OF MASS SPECTROMETRY
J. Mass Spectrom. **33**, 779–795 (1998)

SPECIAL FEATURE
TUTORIAL

Modeling Nucleobase Radicals in the Mass Spectrometer†

František Tureček*
Department of Chemistry, Bagley Hall, Box 351700, University of Washington, Seattle, Washington 98195-1700, USA

Neutralization–reionization mass spectrometry, complemented by *ab initio* and density-functional theory calculations, provides a powerful tool for the investigation of polyatomic radicals relevant to transient intermediates in the process of radiation or chemically induced DNA damage. Precursor ions for analogues of DNA radicals are prepared by gas-phase protonation of nucleobases or their heterocyclic models. The proton affinity of the gas-phase acid is tuned to the topical proton affinity in the substrate molecule to achieve selective protonation. Femtosecond electron transfer imprints the structure of the precursor ion on to that of the radical. Deuterium labeling, collisional activation and variable-time measurements on a microsecond time-scale are used to study unimolecular dissociations of transient heterocyclic radicals and distinguish them from ion dissociations. *Ab initio* and density-functional theory calculations provide energies which are not available from neutralization–reionization experiments. Topical proton affinities, Franck-Condon energies pertinent to vertical electron transfer, radical stabilities and isomerization barriers are used to elucidate the structures and dissociations of isomeric heterocyclic radicals. © **1998 John Wiley & Sons, Ltd.**

KEYWORDS: nucleobase radicals; neutralization–reionization mass spectrometry; modeling; DNA

INTRODUCTION

DNA, the genetic material of most life forms, is susceptible to assault by ionizing radiation, or reactive compounds that are formed in the intracellular fluid or a combination of these two factors. The chemical modifications that occur in the nucleobase, sugar or phosphate structure units are generally referred to as *DNA damage*.[1] DNA damage is distinguished from *DNA mutation*, which alters the nucleobase sequence (the genetic code), but does not chemically alter the building blocks. Chemical modifications in the nucleobase, sugar or phosphate units can have disastrous consequences for the cell. Damage in the nucleobases, adenine (A, **1**), guanine (G, **2**), cytosine (C, **3**) or thymine (T, **4**) disrupts inter-strand base pairing by hydrogen bonds; such damage can be fixed by cellular repair mechanisms. Damage in the sugar or phosphate units can lead to strand breaks that are lethal for the cell.

Owing to the importance of DNA damage for physiological processes as diverse as aging,[2] oxidative stress[3] and radiation damage,[1] the chemistry of DNA damage has been widely studied. It is generally accepted that DNA is attacked by free radicals formed in the intracellular fluid by radiolysis of water, as summarized by von Sonntag.[4] Amongst the radiolytic products formed, the hydroxyl radical is particularly reactive and can attack DNA at the nucleobases to give rise to [DNA + OH]$^{\bullet}$ adducts or abstract a hydrogen atom from the nucleobase or sugar moieties to form [DNA − H]$^{\bullet}$ (Scheme 1). The thermochemistries of these reactions are mostly unknown, although it is presumed that both OH$^{\bullet}$ addition and hydrogen atom abstractions by OH$^{\bullet}$ radicals are exothermic for most C—H bonds. In the gas phase, the branching ratios for H abstractions and OH$^{\bullet}$ additions to aromatic hydrocarbons are usually <0.1,[5] indicating that OH$^{\bullet}$ additions should predominate. Free

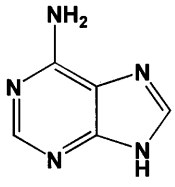

1, A

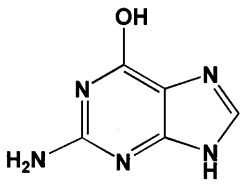

2, G

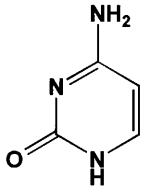

3, C

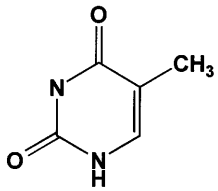

4, T

* *Correspondence to*: F. Tureček, Department of Chemistry, Bagley Hall, Box 351700, University of Washington, Seattle, Washington 98195-1700, USA.

† Dedicated to Dr Vladimír Hanuš on the occasion of his 75th birthday.

Contract/grant sponsor: National Science Foundation.
Contract/grant number: CHE-9412774.
Contract/grant number: CHE-9712570.

CCC 1076–5174/98/090779–17 $17.50

Received 7 July 1998
Accepted 23 July 1998

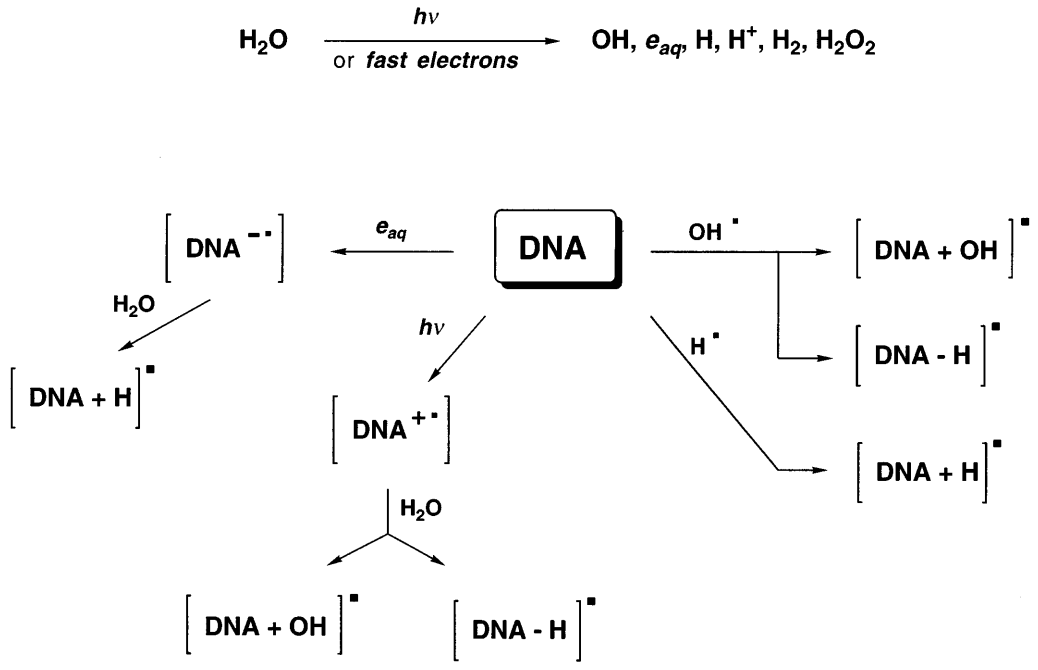

Scheme 1

hydrogen atoms from water radiolysis are thought to add to the nucleobases whereas H abstractions are inefficient.[4] Reactions of DNA with OH$^{\bullet}$ are believed to be more or less random, although it is estimated that most attacks occur on the nucleobases (>70%) rather than on the sugar moieties (<10%).[4] It is unknown whether attacks also occur on the phosphate diester groups.

In addition to the chemically driven mechanisms, DNA radiation damage triggered by direct ionization of DNA has been studied.[6] In the latter mechanism, DNA is ionized directly by photon or electron impact to form cation-radicals (e.g., $\mathbf{G}^{+\bullet}$) or by thermal electron capture to form anion radicals (e.g. $\mathbf{T}^{\bullet -}$, Scheme 1).[6] The importance of the direct ionization mechanism has been stressed by Symons,[6] who argued that the highly reactive OH$^{\bullet}$ radicals formed in the intracellular fluid would not survive long enough to diffuse to the relatively dry cell nucleus and rather would be depleted by reactions with cellular proteins. Since the nucleobases are stacked on the inside of the DNA double strand, a higher proportion of OH$^{\bullet}$ attacks on deoxyribose should be expected.

The DNA cation and anion radicals formed by ionization are thought to react further by proton transfer. The basic anion radicals are rapidly protonated with water to form [DNA + H]$^{\bullet}$. The cation radicals can transfer a proton to a base to form [DNA − H]$^{\bullet}$ or add water and then deprotonate to produce [DNA + OH]$^{\bullet}$ adducts. It has been noted[4] that [DNA + OH]$^{\bullet}$ adducts formed by OH$^{\bullet}$ attack and [DNA + OH]$^{\bullet}$ products from the cation radical-initiated pathway may not be identical, and the same holds for the [DNA + H]$^{\bullet}$ and [DNA − H]$^{\bullet}$ radicals formed by different mechanisms.

The above-mentioned mechanisms point to the decisive role that DNA-derived radicals play in determining the chemistry of DNA damage. Structure elucidation of such reactive intermediates is by no means an easy matter. The presence in DNA of four different nucleobases, the variety of reactive species formed by water radiolysis and the variety of possible sites for attack make it almost impossible to analyze the radical intermediates *in situ*.[4] Therefore, radical reactions have been carried out with synthetic single-strand homo-oligomers (oligo-T, oligo-C, etc.), which contained only one type of nucleobase. Radical intermediates have been probed by both chemical and spectroscopic methods. Trapping with molecular oxygen is one of the chemical methods that converts short-lived C radicals to more stable peroxy radicals.[7] Radical sites have been probed by redox 'titrations' using a series of redox couples of known standard potentials.[8–12] Alternatively, electron spin resonance spectroscopy of samples irradiated in solution or frozen matrices has been used to locate radical centers in some nucleobases.[6,13,14] Although these methods are powerful, they are not free of problems. For example, radical intermediates derived from purine nucleobases (**A** and **G**) are much less amenable to redox titration probes than pyrimidines **C** and **T**.[12] Band broadening is a commonplace problem in ESR studies.[6] In addition, neither redox nor ESR studies are able to study the chemical reactions of DNA radicals other than electron transfer so as to provide structure information on the next generation products. Rearrangements leading to unidentified products have been found to accompany radiolysis.[4,12]

Mass spectrometry has been instrumental in identifying stable products of DNA radiation damage. In the methodology developed by Dizdaroglu *et al.*,[15] DNA is exposed to free radicals generated in solution and then exhaustively hydrolyzed by formic acid to liberate the nucleobases. The latter are trimethylsilylated and analyzed by gas chromatography mass spectrometry. This approach has yielded over 30 hydroxylated products that survived the hydrolytic procedure and contributed to our knowledge of the sites attacked by OH$^{\bullet}$ radicals in solution. However, reactive radical intermediates are lost upon sample work-up and cannot be

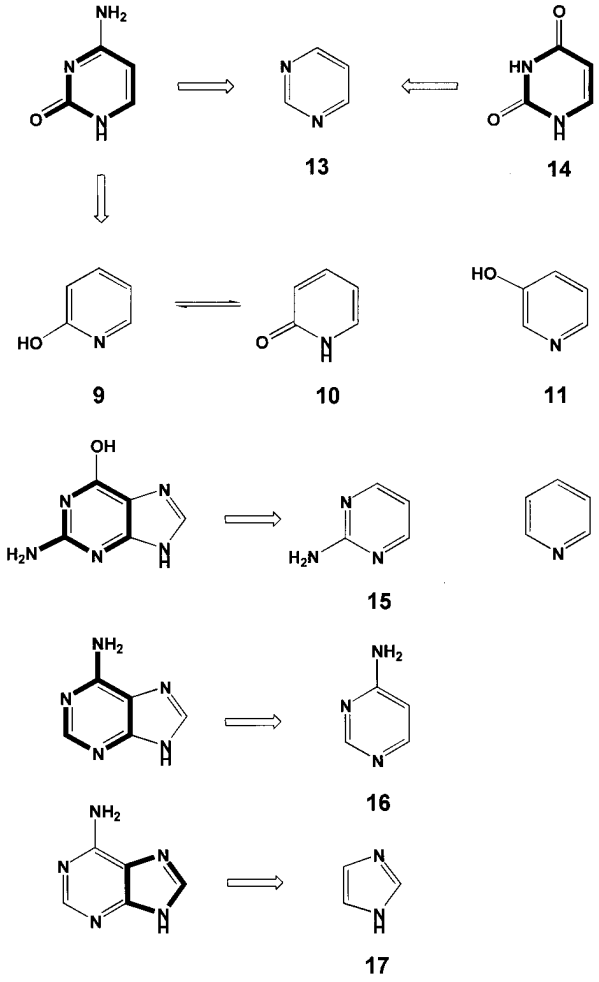

Figure 1. Heterocyclic systems modeling nucleobases. The structure motifs within the nucleobases are highlighted in bold lines.

detected directly. In addition, some of the isolated modified nucleobases undergo rearrangements in the acidic medium, and thus provide only an indirect picture of the modified nucleobases.[15]

From a chemist's point of view, nucleobase-centered DNA radicals are reactive heterocyclic intermediates that can be modeled with simpler derivatives. The structure motifs embedded in the four nucleobases can be represented by pyridine, hydroxypyridines, pyrimidine, hydroxy and aminopyrimidines, imidazole, purine, etc. (Fig. 1). Investigations of transient radicals derived from these simple nitrogen heterocycles thus provide insights into the radical chemistry that can be extrapolated to the more complex polyfunctional nucleobases. Some caution in such extrapolations is in order as highlighted by the recent debate on the role of $OH^{\bullet}$ and carbon-centered radicals in transition metal-induced oxidations.[16–18]

METHODOLOGY

Until the advent of the neutralized beam technique[19,20] and its spin-off, neutralization–reionization mass spectrometry (NRMS),[21–30] neutral intermediates could be studied by mass spectrometry only indirectly as products of ion dissociations.[31,32] Measurements of ionization,[33,34] appearance[35] and collisionally activated dissociation (CAD) threshold energies[36,37] yielded a wealth of energy data for a variety of unstable molecules and radicals. NRMS has been a major advance that allowed one to synthesize unusual and highly reactive neutral molecules and radicals in the gas phase, study their dissociations and analyze the radicals and their dissociation products 'on-line' by tandem mass spectrometry. Heterocyclic radicals relevant to nucleobases are just one of many structure types that have been studied by NRMS.[23–30]

The basic NRMS experiment consists of several sequential steps that rely on the methods of tandem mass spectrometry, as illustrated with the preparation and analysis of imidazolium ions and radicals (Scheme 2). Stable ions of known structure are first prepared, accelerated to kiloelectronvolt kinetic energies and selected by mass to provide a continuous beam of precursor ions. Electron impact, chemical ionization and fast atom bombardment have been used to generate precursor ions in NRMS. The precursor ions enter a collision cell where a fraction undergo electron transfer

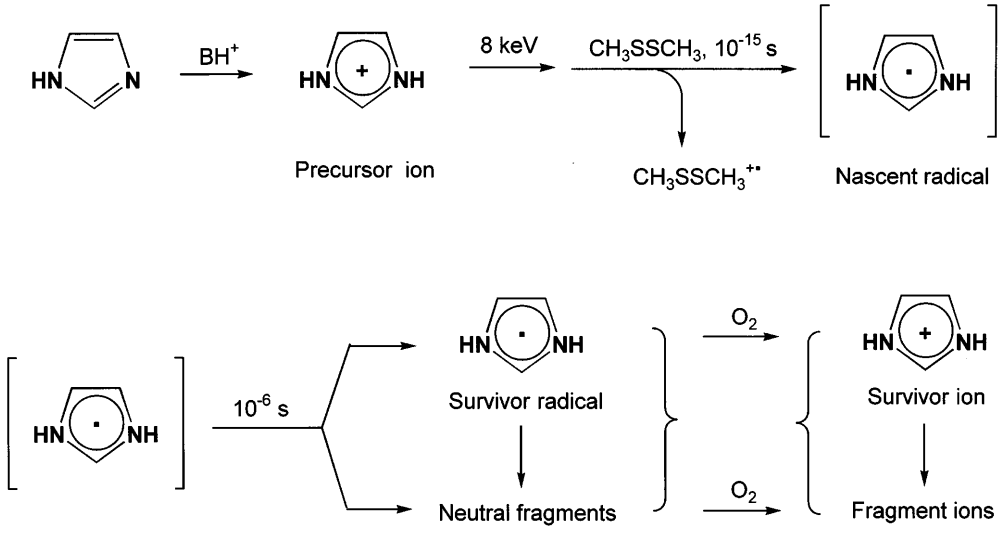

Scheme 2

collisions with a target gas. The electron transfer efficiency depends on the nature and pressure of the collision gas and the precursor ion structure. Typically, a 70–90% range of precursor ion transmittances is employed to favor single-collision conditions. Poisson distribution predicts that out of the precursor ions that have undergone collisions, 83–98% collided only once at 70–90% transmittance. Electron transfer is one of the main processes of ion loss by which fast precursor ions are converted to neutral species. Under the above collision conditions, the neutralization efficiency is about 1–2% of the precursor ion beam.

Two features are important for fast electron transfer that make it a universal method for the preparation of neutral intermediates. First, at keV ion kinetic energies, collisional electron transfer can proceed with virtually any energy balance (ΔE), as expressed by the equation

$$\Delta E = IE_v(\text{target}) - RE_v(\text{ion}) \quad (1)$$

where IE_v is the vertical ionization energy of the target gas and RE_v is the vertical recombination energy (taken as a positive value) for electron capture by the precursor ion. Examples of both exothermic ($\Delta E < 0$) and endothermic ($\Delta E > 0$) electron transfer are well documented.[25] The reason why endothermic electron transfer works at high collision energies is that a small fraction of the non-conserved (center-of-mass) kinetic energy of the ion can be converted to the internal energy of the system and thus make up for the negative energy balance. This feature is of immense practical importance, because stable molecules can be used as electron donors for ions of very low RE_v. In particular, even-electron ions that are used to generate radicals typically have low recombination energies and therefore are not susceptible to reduction under thermal conditions. In spite of the weak dependence on ΔE of the collisional electron transfer, it is advisable to use polarizable atoms or molecules as efficient electron donors. Xe, Hg, $(CH_3)_3N$, *N*,*N*-dimethylaniline, dimethyl disulfide (Scheme 2) and other organic molecules have been used successfully to produce transient radicals from even-electron cations. Even-electron anions are also useful precursors for the formation of radicals.[38,39] Collisional electron detachment is typically accomplished with molecular oxygen as target gas.[25,38]

The second important feature of collisional electron transfer is that it occurs on an extremely short timescale. Interaction between the unoccupied orbitals in the fast ion that accept the electron and the filled orbitals in the donor molecule fades away exponentially with distance. This confines the electron transfer to occurring within a few molecular diameters. For 8 keV ions travelling at 100 000–200 00 m s^{-1} and an interaction path of 10 Å, the interaction times are within 5–10 fs. Within this time frame, molecular rotations are completely frozen, so that the ion–target orientations are fixed and sampled at random.[28] The interaction time for electron transfer is commensurable with the fastest molecular vibrations. For example, a typical O—H stretch of $v = 3600$ cm^{-1} has a vibrational period of 9.3×10^{-15} s.[40] Slower stretching and bending vibrations are practically frozen, so that the relative positions of heavy nuclei in the nascent radical are identical with those in the precursor ion. The net result is that the structure and geometry of the ion are almost exactly copied on to the nascent radical. On the other hand, if the equilibrium geometries of the precursor ion and the radical differ substantially, the latter is formed with distorted bond lengths, angles or dihedral angles. This is equivalent to the radical landing on the wall of a multi-dimensional potential energy well, and the excessive potential energy is then rapidly converted to vibrational excitation (Franck–Condon effect). Franck–Condon (F–C) effects are an important phenomenon in NRMS, because they occur in both neutralization and reionization.[25,41–43] Fortunately, the magnitude of F–C effects can be assessed by *ab initio* calculations to estimate the magnitude and distribution of vibrational excitation in the radicals and ions.[42,43]

Because of its non-resonant nature and femtosecond duration, collisional neutralization offers a non-chemical entry to a wide variety of transient neutral intermediates. Mass spectrometric analysis of radical intermediates and their dissociation products is performed following collisional reionization. Molecular oxygen is the usual reionization target because of its relatively good efficiency and the soft nature of reionization.[44] Under single-collision conditions (70–90% transmittance) the reionization efficiencies are typically of the order of 10^{-3}, making the overall efficiency of NR $\Sigma I_{NR}/I_0 \approx 10^{-5}$. The neutralizing and reionizing collisions introduce some side effects that interfere with NR. While the soft targets used in neutralization are generally inefficient in promoting CAD, neutral fragments from collateral CAD are reionized and detected together with species produced by electron transfer.[45] This contamination by neutral products of precursor ion dissociations is easy to identify from standard CAD spectra. Collisional reionization results in some excitation of the ions formed, due to F–C effects and/or electronic excitation. This excitation causes dissociation of a fraction of the ions formed, so that the products of neutral and post-reionization ion dissociations overlap. A general method for distinguishing neutral and post-reionization ion dissociations relies on the time dependence of these processes (variable-time NRMS).[46,47] Under special circumstances, e.g., neutralization of precursor anions and reionization to cations, $^-NR^+$, a simple subtraction of $^-NR^+$ and charge inversion ($^-CR^+$) spectra provides a rough estimate of neutral dissociations.[39]

One disadvantage of NRMS is that it does not provide energy data for the radical intermediates. NRMS studies are therefore complemented by *ab initio* and/or density functional theory calculations.

INSTRUMENTATION

The capability for NRMS measurements is available on most tandem sector instruments and requires two collision cells in a field-free region following ion selection by mass. For the study of heterocyclic radicals we used the tandem quadrupole-acceleration deceleration mass spectrometer (Fig. 2).[48] This instrument allows one to perform several special experiments, such as neutral col-

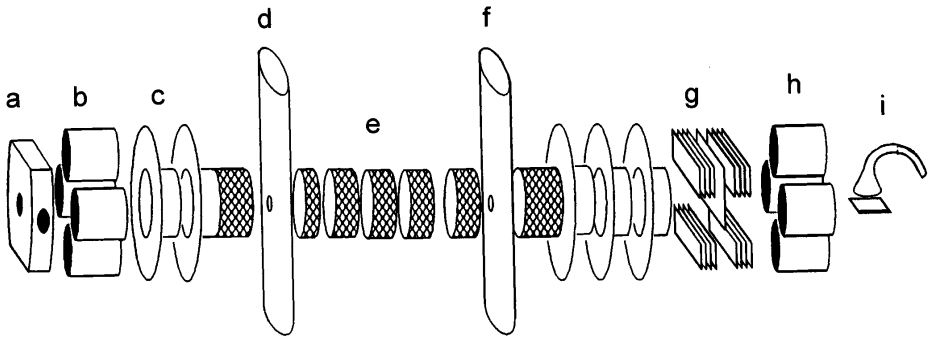

Figure 2. Tandem quadrupole acceleration mass spectrometer for the generation and study of DNA radicals in the gas phase. (a) Ion source; (b) MS-1 quadrupole mass filter; (c) acceleration lens; (d) neutralization collision cell; (e) conduit for variable-time measurements; (f) reionization collision cell; (g) deceleration lens and energy filter; (h) MS-2 quadrupole mass filter; (i) off-axis channeltron electron multiplier.

lisional activation,[49] variable-time measurements,[46,47] neutral photoexcitation[50,51] and photoionization,[52,53] in addition to standard NRMS. An important feature is the capability to distinguish the dissociations of neutral intermediates from post-reionization ion dissociations even if they form chemically identical products.[54] When combined with isotope labeling, this capability provides a powerful mechanistic tool for studying heterocyclic radical chemistry.

PRECURSOR ION STRUCTURES AND RADICAL SYNTHESES

Because of the vertical character of fast electron transfer, the radical synthesis is reduced to the generation of the corresponding gas phase even-electron ion. The general approach to heterocyclic radicals, as illustrated with pyridine (Scheme 3), consists of gas-phase protonation followed by reduction by collisional electron transfer. Formally, this is similar to the electron capture–protonation pathway considered for DNA damage (Scheme 1) except that the steps are interchanged. Both the precursor ion structure and internal energy are of vital importance for the generation and stability of the heterocyclic radical of interest. The precursor ion structure is dictated by the site of gas-phase protonation, which must be known. Also, the energetics of gas-phase protonation are important for assessing the possibility of a rearrangement in the cation formed by exothermic proton transfer. Isomer structures, relative energies and activation barriers for proton migration are often needed for safe assignment of precursor ion structures.

A powerful methodology for the determination of protonation site(s) combines high-level *ab initio* or density-functional theory calculations with experimental probes based on deuterium labeling and NRMS. This two-pronged approach is demonstrated with a simple and straightforward case of protonated pyridine serving as a precursor for the pyridinium radical (**5**).

The calculated topical proton affinities for protonations on N, C-2, C-3 and C-4 in pyridine are shown in Fig. 3. MP2 calculations with the 6–311G(2d,p) basis set have been shown to give very good estimates of proton affinities for nitrogen heterocycles, typically within 5–10 kJ mol^{-1} of reliable experimental values. In line with both chemical intuition and pyridine behavior in solution, the nitrogen atom is by far the most basic site.[55,56] The differences in the topical proton affinities for N and C-2 through C-4 are so large that gas-phase protonation with common chemical ionization reagents, e.g. NH_4^+/NH_3 ($PA(NH_3) = 853$ kJ mol^{-1})[57] or $t\text{-}C_4H_9^+$/isobutane (PA(2-methylpropene) = 801 kJ mol^{-1})[57], occur only at nitrogen. Only very strong gas-phase acids, e.g. CH_5^+/CH_4($PA(CH_4) = 542$ kJ mol^{-1})[57] or H_3^+/H2 ($PA(H_2) = 423$ kJ mol^{-1}),[57] can attack the C-2 through C-4 positions and form tautomeric pyridine cations.

The internal energies of the cations sampled for collisional neutralization are not known exactly, but an educated guess is desirable in order to estimate the internal energy distribution in the radicals to be formed. The ion energy is bracketed from above by the combination of the molecular precursor (pyridine) thermal energy and the protonation exothermicity. However, molecular dynamics of Uggerud[58] indicated that $\leqslant 80\%$ of the protonation exothermicity follows the proton and is deposited in the cation. In the case of a less exothermic protonation, where the acid-base pair remains in contact long enough to distribute the excess energy internally, the excitation is partitioned between the products in the ratio of their heat capacities. The lower bracket for the ion internal energy is given by its thermal vibrational and rotational enthalpy, whose mean values and distribution are readily calculated from the known vibrational frequencies and the ion source temperature. The actual internal energy further depends on the number of collisions that the vibrationally excited ion undergoes with the thermal CI reagent gas and the energy transfer per collision. The mean number of collisions in the CI source ranges between 50 and 100 depending on the gas pressure and ion source potentials. The energy transferred per collision depends on the nature of the collision partners and their internal energy, but it typically ranges between 1.2 and 2.5 kJ mol^{-1}.[59–61] The mean internal energy of a precursor cation produced by exothermic protonation and emerging from the ion source is often hyperthermal with a distribution which is also broader than thermal (Boltzmann). This is an important factor for collisional neutralization. Soft vibrational modes in precursor ions may be substantially excited to $v > 0$ states, and these

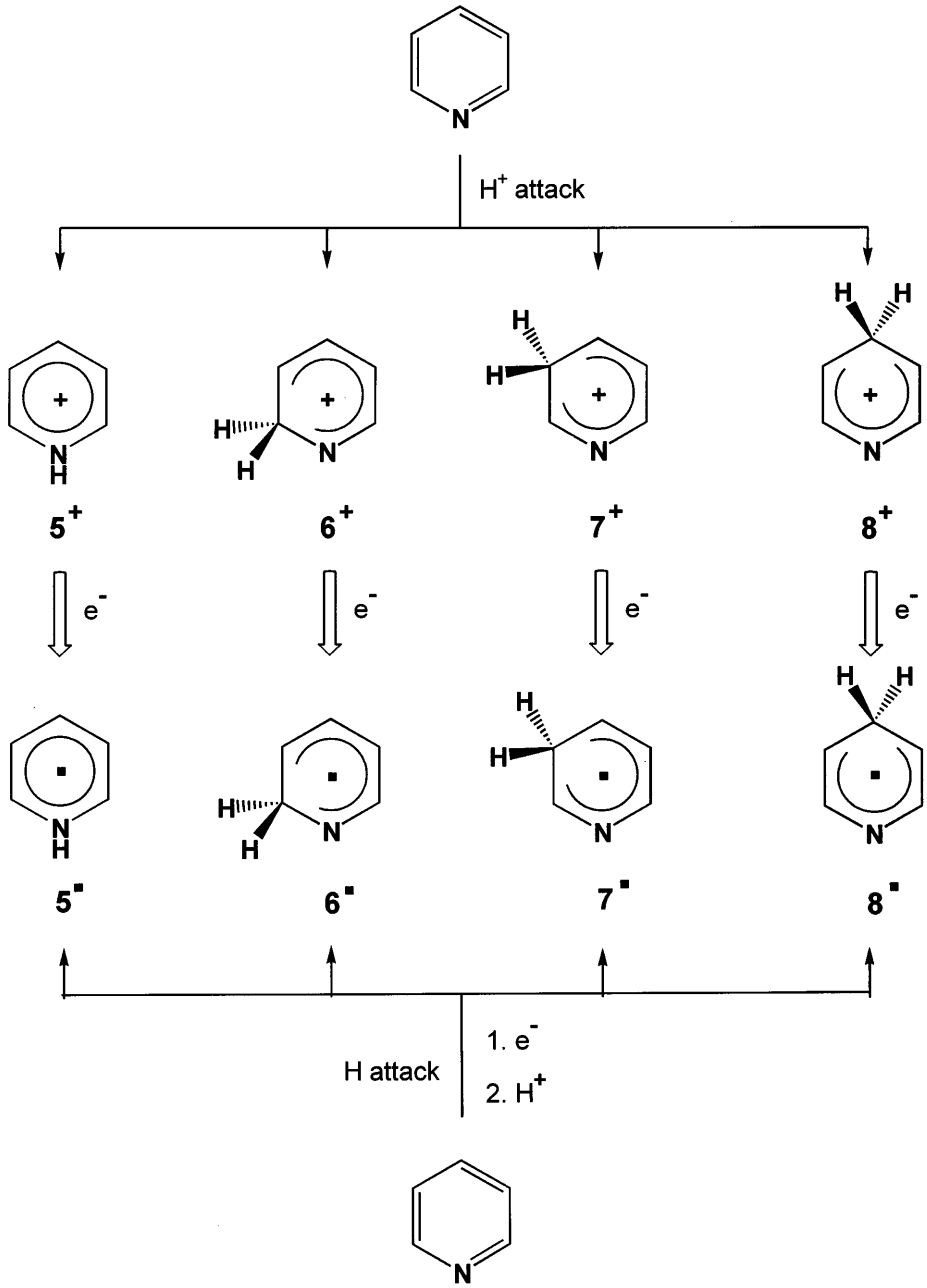

Scheme 3

hot ions have geometries that slightly differ in bond lengths or angles from those in vibrationally relaxed ($v = 0$) ions.

The internal energy of radicals formed by collisional electron transfer is further modified by F–C effects.[62] These arise from a mismatch between the ion and radical equilibrium geometries, as shown for the pyridinium ion and radical (**5**) (Fig. 4). F–C effects result in an increased average excitation in the radicals, but also lead to a broadened distribution of vibrational energies. The magnitude of F–C effects depends on the particular system and can range from modest, e.g. 20 kJ mol^{-1} in **5**,[55] to very large, e.g. 180 kJ mol^{-1} in imidazolinium radicals (**17aH**$^{\bullet}$).[63] It should be noted that F–C energies are not measured experimentally in NRMS and our knowledge of their values relies entirely on *ab initio* or density-functional theory calculations, which sometimes yield different results.

In addition to vibrational excitation, the radicals can be formed in excited electronic states. Collisional electron transfer is not governed by any spin selection rules, so that any of the virtual orbitals in the cationic electron receptor can accept the incoming electron. The probability of the formation of excited states depends on the coupling elements of the interaction Hamiltonian (distorted F–C factors), which are unknown and difficult to calculate.[64] The formation of excited states in collisional transfer has been probed recently by photoexcitation[50,51] and photoionization,[52,53] for a few radical systems, but nothing is known about the formation and properties of excited states in heterocyclic radicals relevant to nucleobases.

The combined effects of precursor ion internal energy, F–C energy, and the threshold energy for radical dissociation determine the fraction of stable radicals to survive the flight time and be reionized. The fraction of

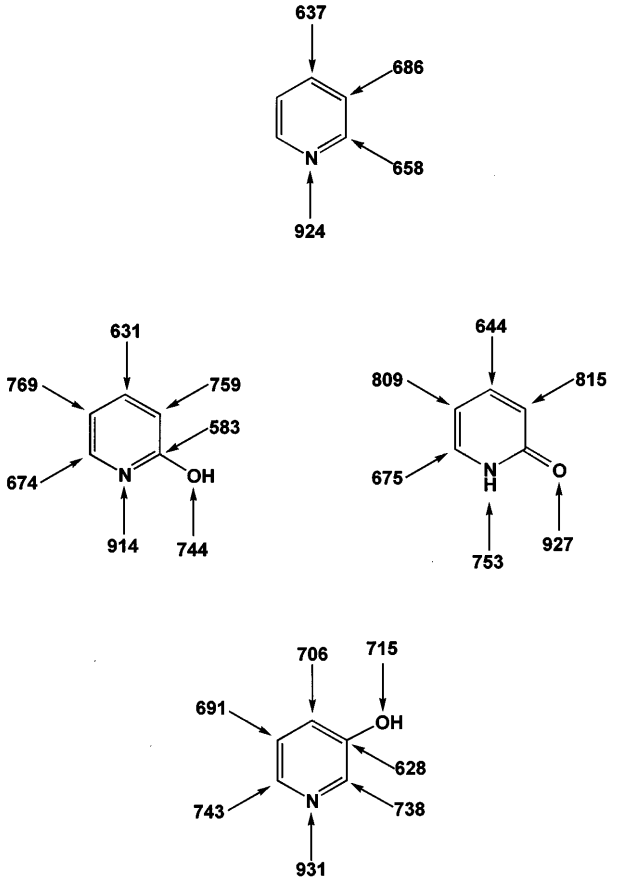

Figure 3. Topical proton affinities (kJ mol^{-1}) in pyridine, 2-hydroxypyridine and 3-hydroxypyridine from MP2/6–311G(2d,p) single-point energies and RHF/6–31G(d,p) zero-point and thermal corrections.

survivor ions which are actually detected is further depleted by post-reionization ion dissociations. However, the latter can be readily gauged from CAD spectra.

RADICAL CHEMISTRY

Pyridinium ions and radicals

Pyridinium radicals **5**˙–**8**˙ (Scheme 3) represent one of the simplest models for studying the relative stabilities and reactivity of heterocyclic radicals relevant to DNA nucleobases. Pyridinium radicals (**5**˙) formed by collisional neutralization of protonated pyridine are stable species that show abundant survivor ions in the NR mass spectra (Fig. 5).[55] The stability of radical **5**˙, expressed as the relative abundance of the survivor $C_5H_6N^+$ ion, depended critically on the vibrational excitation in the precursor. Precursor ions formed by the highly exothermic protonation with CH_5^+ ($\Delta PA = 380$ kJ mol^{-1}) showed substantially lower fractions of surviving radicals than those formed by mildly exothermic protonation with $CH_3NH_3^+$ ($\Delta PA = 23$ kJ mol^{-1}). The radicals dissociated mainly by loss of hydrogen atom to recreate stable pyridine molecules. However, deuterium labeling at both N—D and in the ring positions showed mixed losses of H and D. The loss of D from N—D-labeled pyridinium was enhanced in dissociations of hotter radicals prepared from high-energy precursor ions. Likewise, time-resolved NRMS spectra indicated increased specificity of N–D loss upon

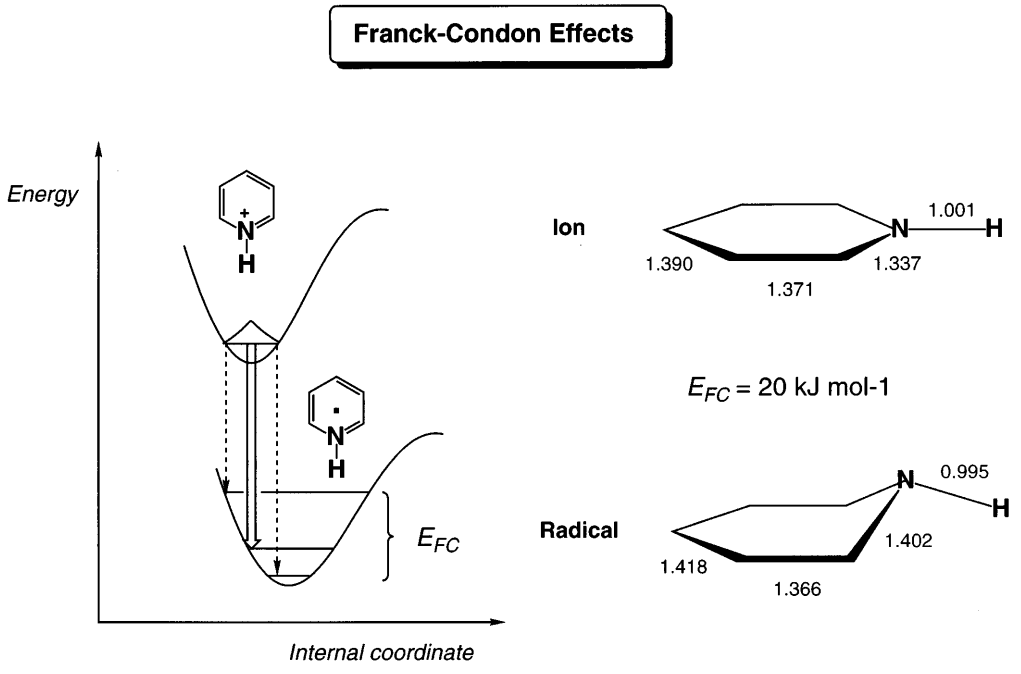

Neutral energy = Ion thermal energy(473 K) + E_{FC} = 19.7 + 20 = **39.7 kJ mol^{-1}**

Figure 4. Franck–Condon energies in vertical neutralization of pyridinium ion $\mathbf{5}^+$.

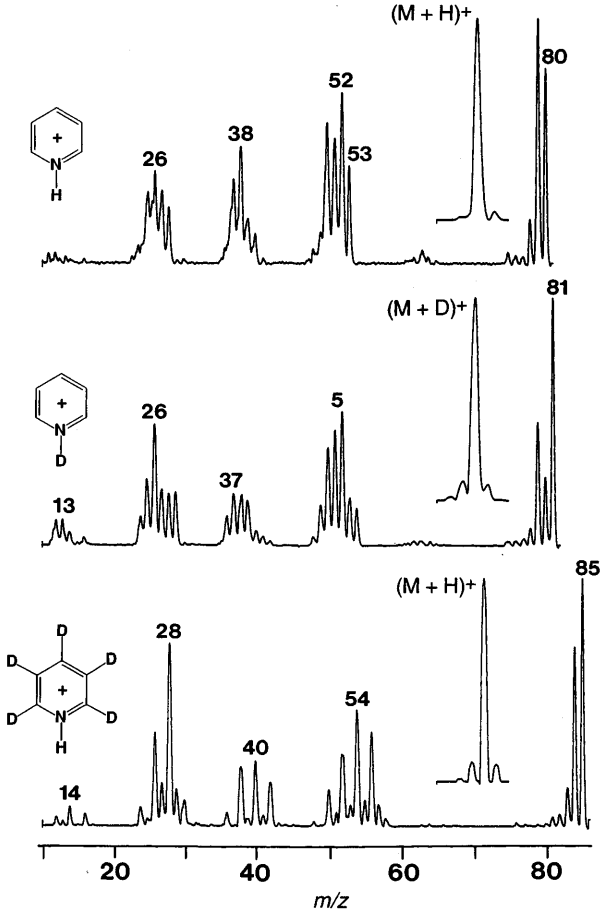

Figure 5. Neutralization (CH_3SSCH_3, 70% T)–reionization (O_2, 70% T) mass spectrum of ion 5^+ and its deuterium-labeled derivatives.

increasing the observation times for dissociations of neutral intermediates. These data allowed unambiguous interpretation that radical dissociations proceeded by specific cleavage of the N—H(D) bonds whereas the post-reionization ion dissociations proceeded with hydrogen scrambling among the N and C-2 through C-6 positions.[55]

The dissociation energetics for pyridinium radicals was obtained from *ab initio* and density-functional theory calculations which quantitatively agreed with experiment. Cleavage of the N—H bond in pyridinium is the lowest energy dissociation pathway (Fig. 6). Orbital analysis of the reactant (**5**˙), transition state and products suggested a smooth reorganization of the frontier orbitals upon N—H bond dissociation. For the reverse reaction, addition of a hydrogen atom to pyridine to give **5**˙, the interaction involved the semi-occupied 1s orbital on the hydrogen atom and the $3b_1$ LUMO of pyridine that evolve into the 14a′ SOMO in **5**. The N—H bond dissociation energies calculated with MP2 and B3LYP and the 6–311G(2d,p) basis set differed, as did the corresponding activation energies (Fig. 6). The 298 K N—H bond dissociation energy in **5**˙ is estimated as 108 kJ mol^{-1} and the energy barrier to H-atom addition to pyridine as 26 kJ mol^{-1}. The other pyridinium isomers 2H (**6**˙), 3H (**7**˙), and 4H (**8**˙) were also bound but were less than **5**˙ (Fig. 7). The differences between the relative energies of isomeric radicals are much smaller than those for the isomeric cations (Fig. 3). The general trend, which is corroborated by MP2 and B3LYP calculations for several heterocyclic systems, shows substantially smaller differences in the radical relative stabilities as compared to ion stabilities. In addition, reversals in the radical relative stabilities occur for some systems as discussed below.

The calculations also yielded thermochemical data for the addition and abstraction reactions in the pyridine model system.[65] Figure 7 summarizes the calculated 298 K reaction enthalpies (averaged over MP2 and B3LYP/6-311G(2d,p) calculations) for the formation of pyridinium and pyridyl radicals. Additions of H˙ to give **5**˙–**7**˙ are highly exothermic regardless of the site of attack. By contrast, hydrogen atom abstractions by H˙ are substantially endothermic for all positions in pyridine. This indicates that hydrogen atom additions should be the energetically preferred modes of pyridine reacting with hydrogen atoms. It is unknown whether the H-abstraction reactions in pyridine have activation barriers above the endothermic energy thresholds.

Hydroxypyridinium ions and radicals

Introduction of a hydroxy group into the pyridine nucleus has some major effects on the ion and radical relative energies and reactivity. The parent 2-hydroxypyridine system is known to consist of two tautomeric forms, e.g. **9** and (1H)-2-pyridone (**10**) (Scheme 4), which have comparable stabilities in the gas phase[66] and have been studied extensively as nucleobase models.[67] Theoretical calculations mostly predicted **9** to be the more stable isomer ($\Delta H_{r,298}(\mathbf{9} \rightarrow \mathbf{10}) = 5$–$6$ kJ mol^{-1}), although both the magnitude and the sign of the energy difference depended on the computational method used. QCISD(T), MP2[68] and DFT calculations[68,69] gave **9** as the most stable isomer, whereas CASSCF calculations favored **10**.[70] Spectroscopic studies of the (**9** + **10**) system in the gas phase favored **9** as the predominant and hence more stable tautomer.[71,72] 3-Hydroxypyridine exists as a single tautomer **11**, which was calculated to be about 40 kJ mol^{-1} less stable than **9**.

Protonation of hydroxypyridines, followed by collisional neutralization, provides access to radicals that can be viewed as intermediates of either hydrogen atom attack on hydroxypyridines or hydroxyl radical attack on pyridine. The structure of radicals prepared by NRMS depend on (1) the position of the hydroxyl group in the precursor molecule, (2) the tautomer composition and (3) the protonation site.

The protonation sites in the 2-hydroxypyridine system depend on the topical proton affinities and the gas-phase acid used.[65] The topical proton affinities of both tautomers are shown in Fig. 3. Protonation with mild acids, e.g., NH_4^+ or $t\text{-}C_4H_9^+$, forms exclusively the most stable ion **9aH**$^+$ from both tautomers **9** and **10** (Scheme 4). Stronger acids, e.g., H_3O^+, can attack positions C-3 and C-5 in both **9** and **10** in addition to the nitrogen and oxygen atoms to form a mixture of ion isomers. Very strong acids, e.g., CH_5^+, can exothermically protonate any position in **9** and **10**. Which of the energetically accessible positions is (are) protonated

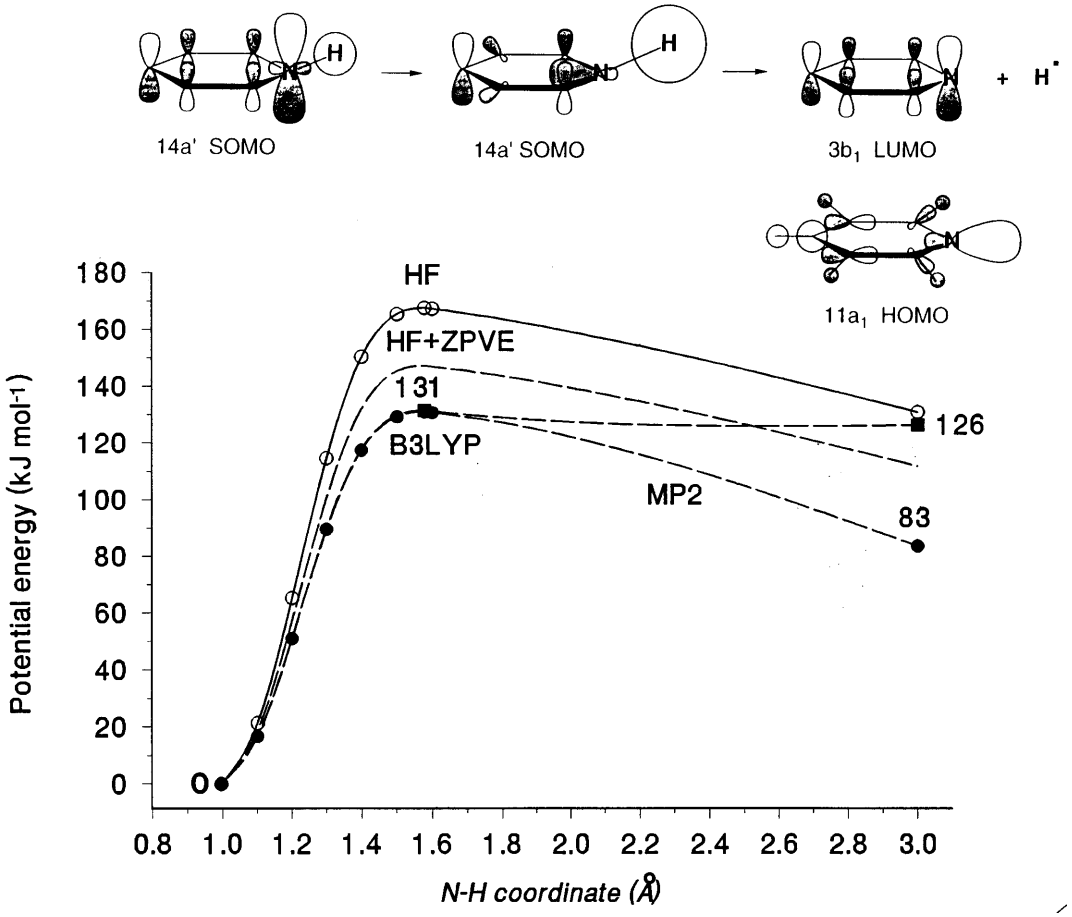

Figure 6. Potential energy profile for N—H bond dissociation in 5•.

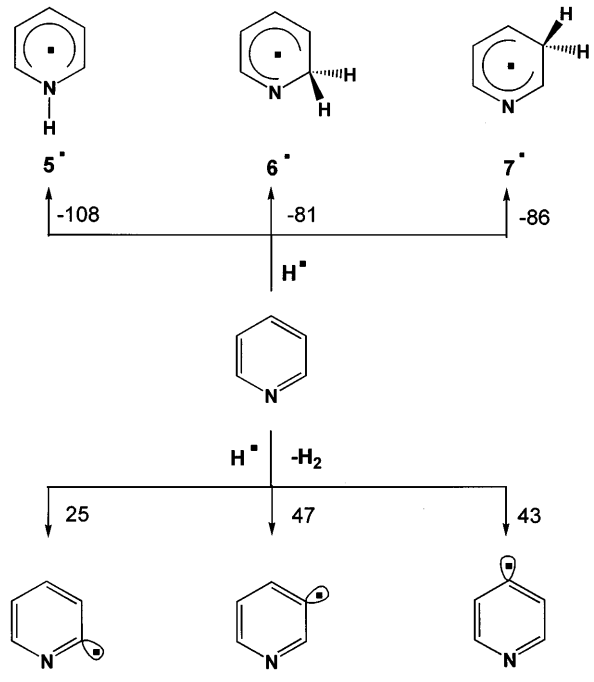

Figure 7. Relative 298 K enthalpies for hydrogen atom additions and abstractions in pyridine. Averaged MP2 and B3LYP/6–311G(2d,p) relative energies with HF/6–31G(d,p) zero-point and thermal corrections.

by strong gas-phase acids depends on the proton transfer kinetics.[73] Although the rate constants for proton transfer correlate with the reaction free energy,[73] local dipole moments in a polyfunctional molecule may also affect the relative rates of protonation at different sites, provided the proton transfer is exothermic and therefore energetically favored. In addition, under the conditions existing in the chemical ionization ion source, the less stable ion tautomers may exothermically protonate

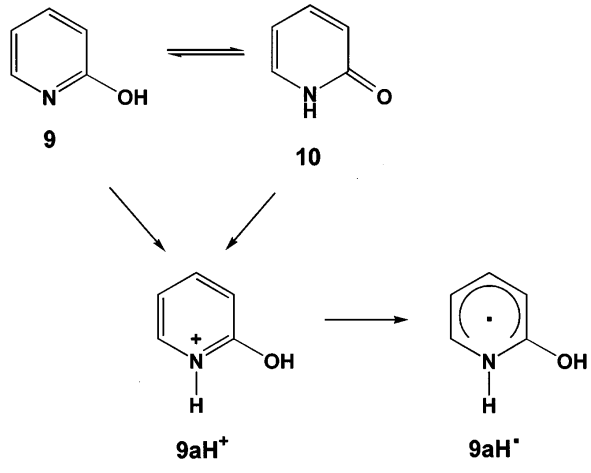

Scheme 4

the precursor molecules, which are always present in large excess. This shake-up by successive protonations is thought to eventually yield the most stable isomer **9aH**$^+$. The composition of ion mixtures produced by exothermic protonation of polyfunctional molecules depends on experimental conditions (reagent and analyte partial pressure, ion residence time) and the proton transfer kinetics. In particular, activation barriers for proton transfer between tautomers can hinder ion isomerization by ion–molecule reactions. It is clear that the population of ion tautomers produced by exothermic protonation will determine the initial population of radicals formed by femtosecond electron transfer. In addition, the radical population must be affected by the relative neutralization cross-sections of the ion isomers, which are usually unknown.

The 2-hydroxypyridinium radical (**9aH**$^{\bullet}$) produced by collisional neutralization of **9aH**$^+$ is a stable species as revealed by experiment and confirmed by theory.[65] The NR mass spectrum of **9aH**$^+$ showed an abundant survivor ion. The radical dissociates mainly by loss of a hydrogen atom. Other dissociation products observed in the NRMS spectrum can be attributed to post-reionization dissociations of **9aH**$^+$ and **9**$^{+\bullet}$ or **10**$^{+\bullet}$ as deduced from the CAD spectra of these ions. The radical and post-reionization ion dissociations were further distinguished by combination of deuterium labeling, CAD, NR, NCR and variable-time NR spectra. These experiments showed that radical dissociations involved specific (>90%) cleavages of the O—H and N—H bonds to form **9** and **10**. The apparent loss of hydrogen atoms from other ring positions was due to hydrogen scrambling in reionized **9aH**$^+$ that preceded dissociation by loss of H$^{\bullet}$. The unimolecular chemistry of **9aH**$^{\bullet}$ was thus established unambiguously.

One disadvantage of the protonation–neutralization strategy is that the structure of the ion isomer to be formed is dictated by the topical proton affinity in the precursor molecule. The other isomers, if inaccessible experimentally, must be investigated by theoretical calculations that provide relative energies, isomerization barriers and dissociation energies. The energetics in the 2-hydroxypyridinium radical system are shown in Scheme 5. Addition of OH$^{\bullet}$ to the C-2 position in pyridine is exothermic to form radical **9bH**$^{\bullet}$. The latter has enough internal energy to dissociate by C-2—H bond cleavage leading to **9** and a hydrogen atom ($\Delta H_r = 34$ kJ mol^{-1}). However, 1,2-hydrogen migrations in **9bH**$^{\bullet}$ can produce **9aH**$^{\bullet}$ and **9cH**$^{\bullet}$ by exothermic isomerizations. The latter can further rearrange to another stable radical isomer **9dH**$^{\bullet}$. The dissociation of **9aH**$^{\bullet}$ to **9** and a hydrogen atom is endothermic by 74 kJ mol^{-1} (Scheme 5). Assessing the kinetics of the competitive rearrangements and dissociations requires calculations of transition states. These are difficult in radical systems because of the imperfect treatment of correlation energy and, in the case of perturbational calculations, substantial spin contamination. Fortunately, NRMS measurements of deuterium-labeled radicals provide the complementary information at the qualitative level. Dissociations of O,N-deuterium labeled **9aD**$^{\bullet}$ proceeded with predominant (>90%) loss of D. This implied that structures (**9cH**$^{\bullet}$–**9fH**$^{\bullet}$) that could have caused H,D scrambling were not involved in the dissociation and must have been separated from **9aH**$^{\bullet}$ by substantial energy barriers.

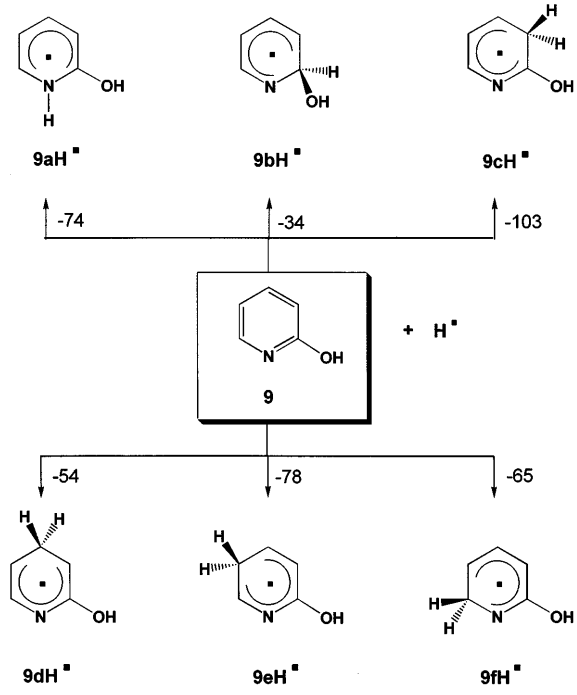

Scheme 5

The 3-hydroxypyridinium system (**11H**$^{\bullet}$) does not have any analogy among the purine and pyrimidine nucleobases and was studied as a non-tautomeric model of a heterocyclic radical.[74] Gas-phase protonation of **11** was predicted by MP2 and B3LYP calculations to occur on the nitrogen atom, which showed the greatest proton affinity (Fig. 3). Neutralization of ion **11aH**$^+$ yielded radical **11aH**$^{\bullet}$ as a stable species that showed a substantial survivor ion in the NR mass spectrum. The relative abundance of the survivor ion decreased with the increasing internal energy of the precursor ion when the latter was formed by increasingly exothermic protonations with NH_4^+, t-$C_4H_9^+$, H_3O^+ and CH_5^+. Dissociation of **11aH**$^{\bullet}$ proceeded predominantly by loss of the N-bound hydrogen atom, as distinguished by complementary deuterium labeling on N and in the OH group. Radical **11aH**$^{\bullet}$ is the most stable isomer among the 3-hydroxypyridinium isomers. The calculated relative energies showed that an OH$^{\bullet}$ attack at C-3 in pyridine was 59 kJ mol^{-1} exothermic to yield radical **11bH**$^{\bullet}$. The latter can dissociate by loss of H$^{\bullet}$ to form **11**, or rearrange by 1,2-hydrogen migrations to form **11cH**$^{\bullet}$ and **11aH**$^{\bullet}$. The absence of H/D exchange in dissociating **11aH**$^{\bullet}$ clearly indicated that the energy barrier to hydrogen migration was greater than that for N—H bond cleavage (Scheme 6).[74]

Pyrimidinium, uracil and thymine ions and radicals

The protonation–neutralization strategy was applied to pyrimidine (**13**), uracil (**14**) and thymine (**4**) with the goal of generating the corresponding radicals and study their gas-phase stabilities and dissociations. Standard CI reagents (NH_4^+, t-$C_4H_9^+$, H_3O^+) protonate pyrimidine exclusively on nitrogen, as predicted by *ab initio* calcu-

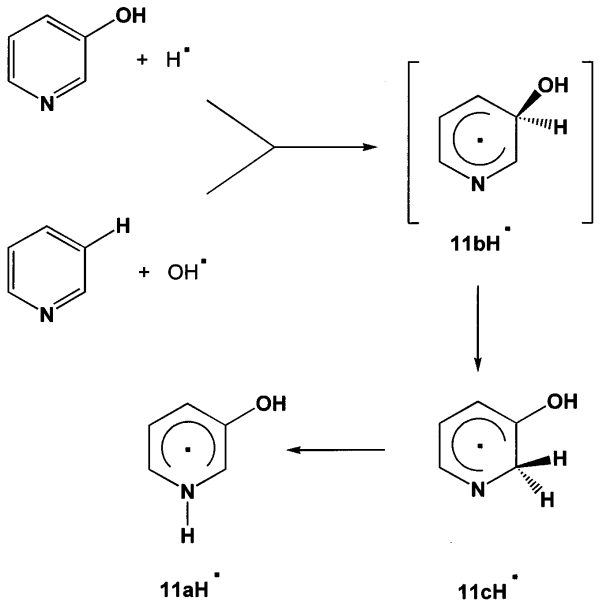

Scheme 6

lations of topical proton affinities (Fig. 8).[75] The pyrimidinium (**13aH**•) is a stable species when generated by collisional electron transfer from ion **13aH**$^+$ (Scheme 7). The main dissociation is cleavage of the N—H bond to form **13**, as confirmed by deuterium labeling. The stability of **13aH**• depended mainly on the internal energy of the precursor ion. For example, NRMS of ion **13aH**$^+$, which was prepared by exothermic protonation with H_3O^+ ($\Delta PA = 192$ kJ mol^{-1}), resulted in a four-fold lower relative abundance of reionized **13aH**• than NRMS of **13aH**$^+$ from less exothermic protonation with NH_4^+ ($\Delta PA = 29$ kJ mol^{-1}). Franck–Condon energies in vertical neutralization of **13aH**$^+$ are relatively small (22–23 kJ mol^{-1}) and alone cannot cause radical dissociation.[75]

Similar conclusions were reached regarding the functionalized pyrimidines uracil (**14**) and thymine (**4**). Protonation–neutralization of both **14** and **4** produced stable radicals, **14H**• (Scheme 8) and **4H**•, respectively, that yielded substantial survivor ions in the NR mass spectra. In addition to hydrogen atom loss, which was typical of pyridinium and pyrimidinium radical dissociations, **14H**• and **4H**• showed abundant ring cleavage dissociations, as illustrated with the NR mass spectrum of **14H**• (Fig. 9). The dissociation energetics of **14H**• and **4H**• are unknown, and their elucidation by high-level *ab initio* calculations will require substantial effort and resources because of the size of these systems.

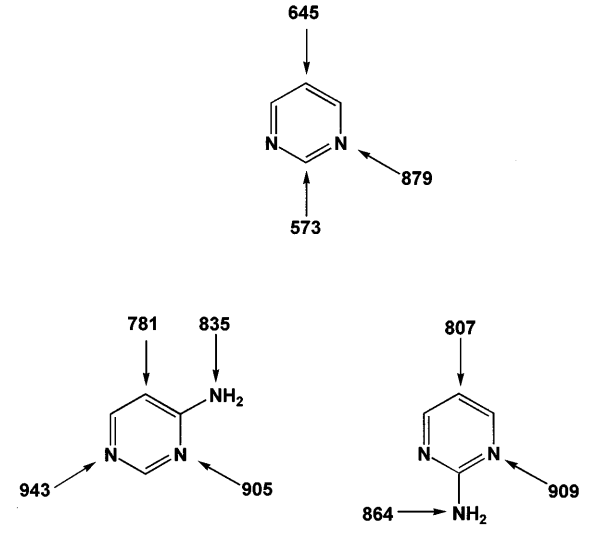

Figure 8. Topical proton affinities (kJ mol^{-1}) in pyrimidine (**13**), 2-aminopyrimidine (**14**) and 4-aminopyrimidine (**15**) from MP2/6–311G(2d,p) single-point energies and RHF/6–31G(d,p) zero-point and thermal corrections.

Aminopyrimidinium ions and radicals

2-Aminopyrimidine (**15**, Scheme 9) and 4-aminopyrimidine (**16**, Scheme 10) represent simple heterocyclic compounds that were used to generate and investigate radicals relevant to guanine and cytosine.[75] The presence of the amino group in **15** and **16** affects the protonation thermochemistry in two ways. First, the amino group is sufficiently basic to be protonated competitively under CI conditions. Second, the electron-donating effects of the amino group increase the topical proton affinities in the ring and make the ring positions amenable to protonation. The calculated topical proton affinities in **15** and **16** are summarized in Fig. 8. Mild gas-phase acids (NH_4^+ and t-$C_4H_9^+$) protonate **15** at both ring nitrogens and the amino group in a 2:1 ratio to form a mixture of ions **15aH**$^+$ and **15bH**$^+$ (Scheme 9). The ring carbon atoms are not protonated. The radicals formed by collisional neutralization of **15aH**$^+$ and **15bH**$^+$ showed a substantial fraction of stable species that yielded survivor ions following collisional reionization. To distinguish which of **15aH**• and **15bH**• was stable required *ab initio* calculations of the pertinent structures. Radical **15aH**• is bound in its equilibrium structure and stable when formed by vertical neutralization of **15aH**$^+$. The electron-donating 2-amino group does not destabilize **15aH**• compared with the parent pyrimidinium (**13H**•). Radical **15bH**• is much less stable than **15aH**• and is likely to dissociate rapidly by cleavage of one of the N–H bonds.

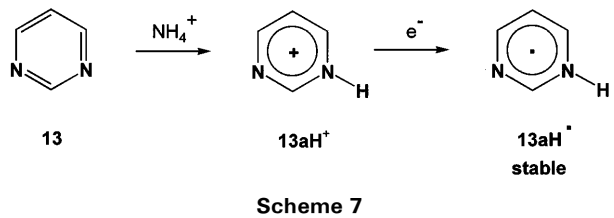

Scheme 7

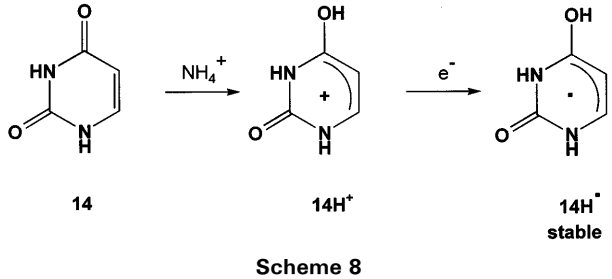

Scheme 8

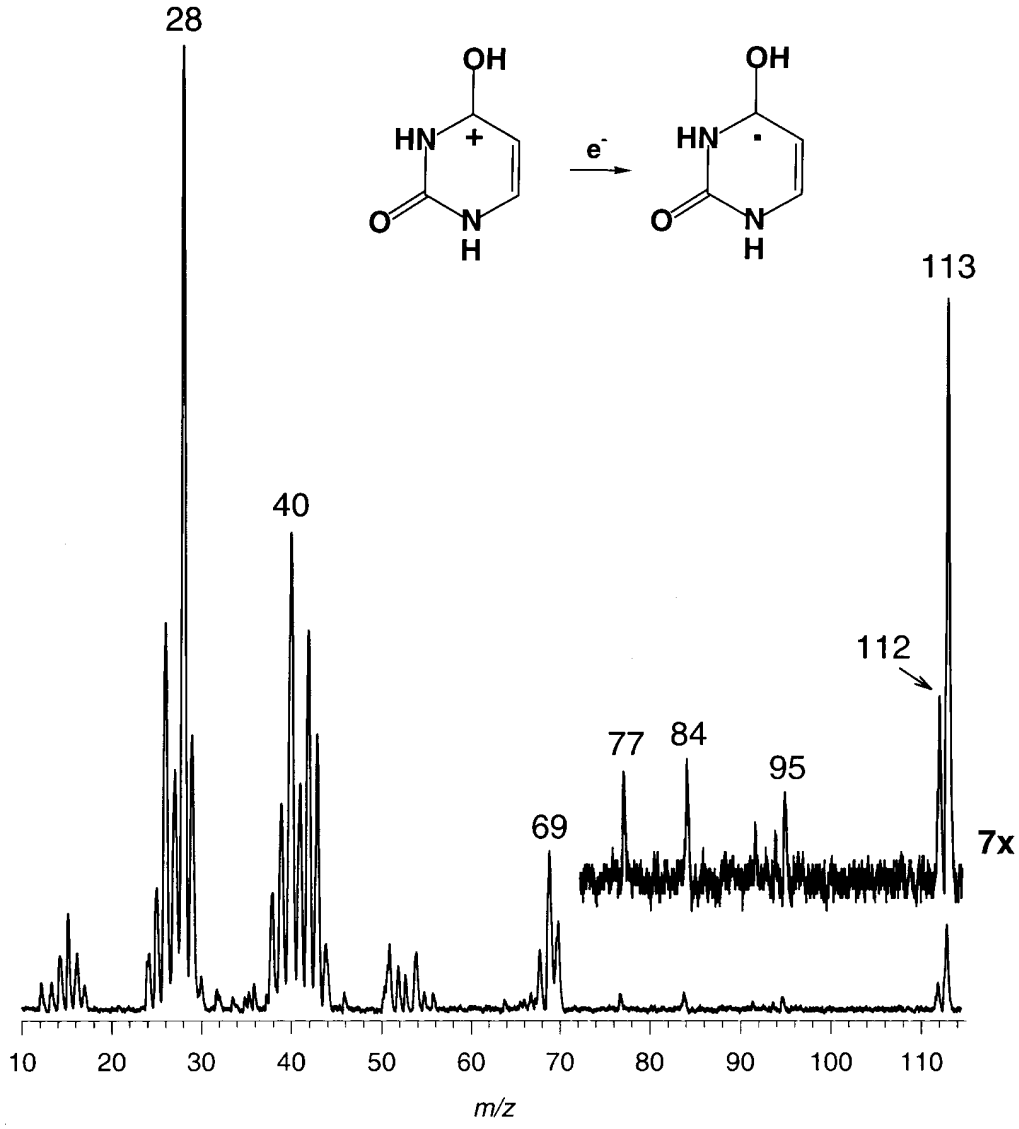

Figure 9. Neutralization (CH_3SSCH_3, 70% T)–reionization (O_2, 70% T) mass spectrum of protonated uracil.

Protonation of **16** forms three tautomeric ions, **16aH**$^+$, **16bH**$^+$ and **16cH**$^+$, which served as precursors for 4-aminopyrimidinium radicals (Scheme 10). Species **16aH**$^\cdot$ and **16bH**$^\cdot$ are standard heterocyclic radicals which are fairly stable when formed by collisional neutralization. The NR mass spectrum of protonated **16** showed a prominent survivor ion by reionization of the stable radical intermediate.[75] The calculated dissociation energies of the N-1—H and N-3—H bonds in **16aH**$^\cdot$ and **16bH**$^\cdot$ are very similar and range between 68 and 76 kJ mol^{-1}. Interestingly, the N-1—H and N-3—H bond dissociations have energy barriers of 105–107 kJ mol^{-1}, which increase the kinetic stability of **16aH**$^\cdot$ and **16bH**$^\cdot$. Conversely, the activation barriers to the reverse hydrogen atom addition to **16** (29–40 kJ mol^{-1}) are sufficiently large to slow the reaction under thermal conditions (Fig. 10).[76]

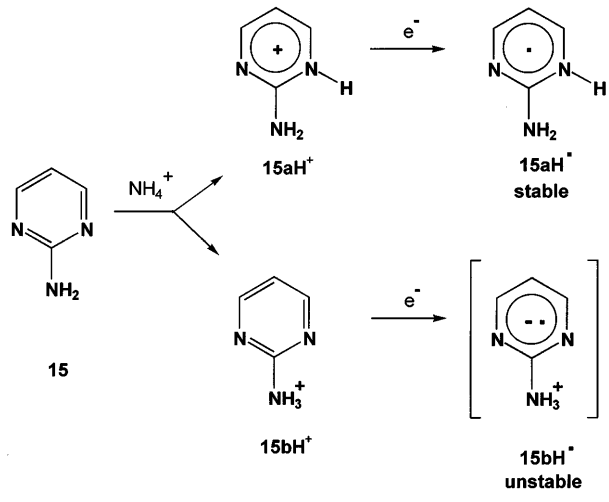

Scheme 9

Radical **16cH**$^\cdot$, arising by neutralization of the ammonium ion **16cH**$^+$, is an interesting species which formally resembles hypervalent ammonium radicals.[75] However, **16cH**$^\cdot$ can be better represented as a zwitterionic species consisting of a positively charged NH_3^+ group and a negatively charged pyrimidine anion radical. Radical **16cH**$^\cdot$ exists in a shallow energy minimum, which is separated from exothermic dissociation to **16** and H$^\cdot$ by a small activation barrier of 22 kJ mol^{-1}. It should be noted that formation of radical

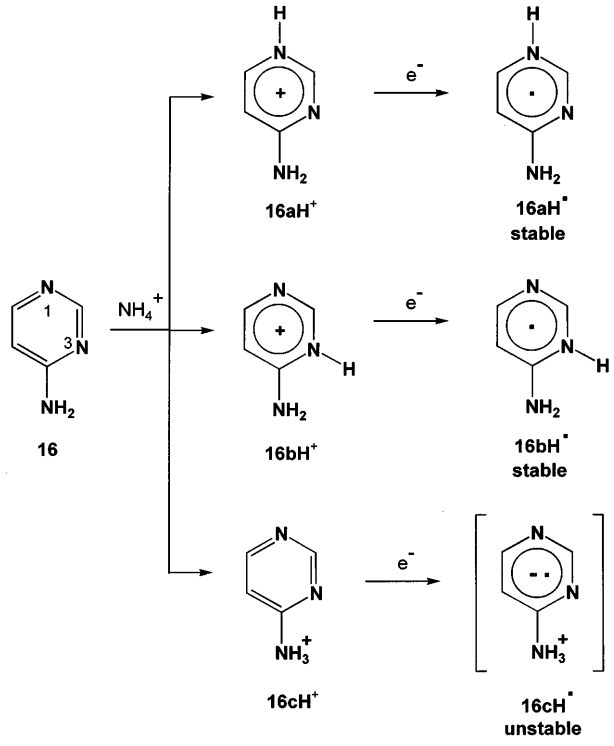

Scheme 10

16cH• by a bimolecular reaction, e.g. attack of a hydrogen atom at the NH_2 group in **16**, would be severely hampered by the reaction endothermicity ($\Delta H_{r,0} = 58$ kJ mol^{-1}).[76]

Caveats in computations of heterocyclic radicals

It is worth noting that calculations of heterocyclic radicals yield relative energies that depend strongly on the method and basis set used. Density-functional theory methods, e.g., Becke's B3LYP,[77,78] tend to overstabilize organic radicals relative to closed-shell molecules and thus provide dissociation energies which are 20–30 kJ mol^{-1} too high.[79] This overestimation varies very little with the size of the basis set, e.g., for the split-valence basis sets 6–31 + G(d,p), 6-311G(2d,p) and 6-311 + G(2d,p) that were used for the above heterocyclic radicals.[75,76] In contrast, perturbational *ab initio* methods, e.g. MP2, suffer from spin contamination problems, which are not removed completely by standard spin annihilation procedures.[62,63,75] MP2 dissociation energies in heterocyclic radicals are therefore underestimated by 20–30 kJ mol^{-1} and improve only slowly upon increasing the basis set. Composite procedures according to the equation

$$\begin{aligned}\text{QCISD(T)/6–311 + G(2d,p)} &\approx \text{QCISD(T)/6–31G(d,p)} + \text{PMP2/6–311} \\ &\quad + \text{G(2d,p)} - \text{PMP2/6–31G(d,p)} \end{aligned} \quad (2)$$

give more reliable data, because the quadratic configuration interaction (QCISD(T)) energy is spin-contamination free, and the residual spin contamination in the projected MP2 energies (PMP2) cancel out. However, these calculations are expensive for large

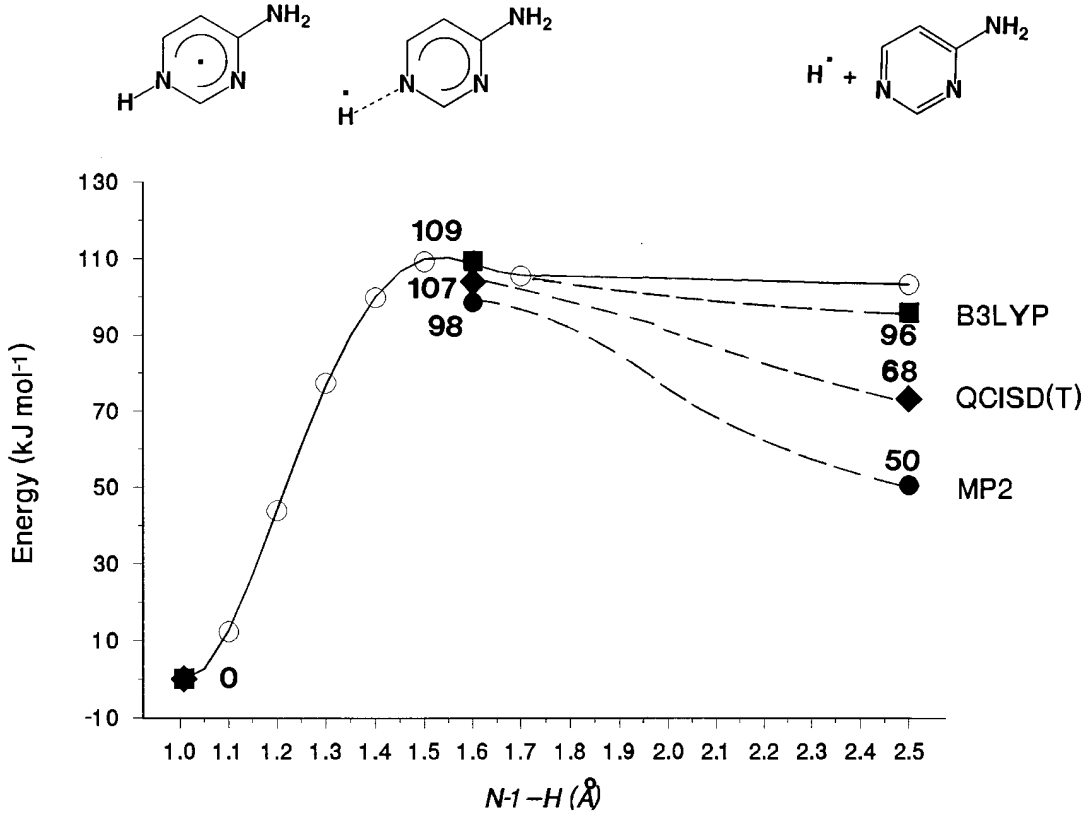

Figure 10. Potential energy profile for the dissociation of the N-1—bond in **16aH•**. Single-point energies (kJ mol^{-1}) calculated with the 6–311 + G(2d,p) basis set and B3LYP/6–31 + G(d,p) zero-point corrections.

open-shell systems such as **16aH**$^{\bullet}$–**16cH**$^{\bullet}$.[76] Interestingly, the errors inherent to the MP2 and B3LYP calculations are almost exactly compensated upon averaging the energies.[80] This simple empirical procedure thus provides a shortcut to good quality relative energies.

Imidazolium and pyrrylium ions and radicals

The imidazole ring is a structure motif which is built in the purine skeleton of adenine and guanine. Radical attack on **A** and **G** often results in the imidazole ring cleavage.[4,15] The intrinsic properties of imidazole (**17**) radicals were therefore of interest and were addressed by NRMS.[63] Imidazole is protonated in the gas phase on the imine nitrogen atom, which is by far the most basic site (Fig. 11).[63] The structure of the gas-phase ion **17aH**$^{+}$ is therefore well defined. Formation of radical **17aH**$^{\bullet}$ by vertical neutralization accompanied by 99% dissociation by loss of hydrogen and ring cleavage, such that the survivor ion is very weak in the NR mass spectrum.[63] This contrasts with the behavior of other heterocyclic radicals, pyrrylium,[63] pyridinium[55] and pyrimidinium,[75] which all showed substantial fractions of non-dissociating radicals (see above). Interestingly, deuterium labeling in **17aH**$^{+}$ showed partial exchange of the N—(H,D) and C-2—(H,D) hydrogen atoms in the intermediate radical **17aH**$^{\bullet}$, which occurred prior to or in the course of dissociation by N—(H,D) bond cleavage. The energetics of the radical formation and dissociations were therefore of interest. *Ab initio* and density-functional theory calculations revealed that **17aH**$^{\bullet}$ was only weakly bound against dissociation to imidazole and hydrogen atom, which required $\Delta H_{r,298} = 30$ kJ mol^{-1} after averaging the MP2 and B3LYP/6–311G(2d,p) energies. Vertical neutralization of **17aH**$^{+}$ is accompanied by large F–C effects that result in vibrational excitation of the **17aH**$^{\bullet}$ radical formed (Fig. 12). The hot radical dissociates by N—H bond cleavage to form imidazole, but without scrambling the N—H and C—H hydrogen atoms. Concurrently, **17aH**$^{\bullet}$ can rearrange by exothermic isomerization to the more stable radical **17bH**$^{\bullet}$. The latter is a bound species when formed by vertical reduction of its ion **17bH**$^{+}$ (Fig. 12). However, following isomerization from **17aH**$^{\bullet}$, radical **17bH**$^{\bullet}$ has a sufficient internal energy to dissociate to **17** by loss of either C-2—H hydrogen atoms, which thus become indistinguishable. The existence of intermediate **17bH**$^{\bullet}$ explains the partial scrambling of the N—H and C-2—H hydrogen atoms in dissociating **17aH**$^{\bullet}$.

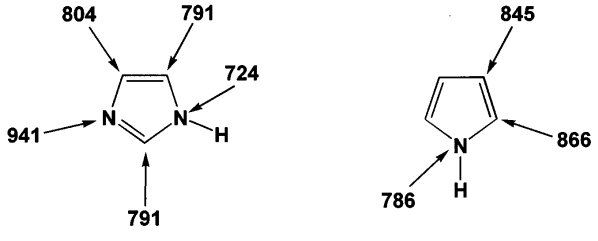

Figure 11. MP2/6–311G(2d,p) calculated topical proton affinities (kJ mol^{-1}) in imidazole and pyrrole.

Phosphorane radicals

Transient radicals derived from phosphate esters are perhaps the most difficult ones to detect and study in solution. It is clear, however, that detection of phosphate radicals upon DNA irradiation would unambiguously indicate that strand breaks occurred upon DNA damage. NRMS allows for a straightforward generation of oxygenated phosphorus radicals via two routes.[81] First, electron impact ionization of trialkyl phosphates, $(RO)_3P{=}O$, R = ethyl and higher, results in facile dissociation by stepwise elimination of an alkenyl radical and two alkene molecules to form an abundant $P(OH)_4^+$ ion at m/z 99 (**18**$^{+}$, Scheme 11). Ion **18**$^{+}$ was characterized by the metastable ion and CAD spectra and its structure was inferred from *ab initio* calculations which showed it to be the most stable $H_4PO_4^+$ isomer. Cation **18**$^{+}$ served as a precursor for the generation of tetrahydroxyphosphorane, $P(OH)_4^{\bullet}$, **18**$^{\bullet}$. Second, protonation of trimethyl phosphate gave rise to the hydroxytrimethoxyphosphonium ion (**19**$^{+}$), which had the structure suitable for the generation of the hydroxytrimethoxyphosphoranyl radical **19**$^{\bullet}$ by collisional neutralization. A surprising result of the NR mass spectra of **18**$^{+}$ and **19**$^{+}$ was the absence of both survivor ions and stable product molecules formed by cleavages of the P—O bonds, e.g., $P(OH)_3$, $P(OH)(OCH_3)_2$ and $P(OCH_3)_3$. Interpretation of the spectrum of **18**$^{\bullet}$ was aided by *ab initio* calculations that revealed several unusual features. Radical **18**$^{\bullet}$ is a stable species that exists as several stereoisomers[81,82] that interconvert by configurational inversion at the tetracoordinated phosphorus atom known as the Berry pseudorotation.[82] Dissociations of **18**$^{\bullet}$ by O—H and P—O bond cleavages must overcome activation barriers, calculated at 90 and >160 kJ mol^{-1}, respectively, which stabilize the radical kinetically (Fig. 13). However, vertical neutralization of **18**$^{+}$ is accompanied by very large F–C effects which deposit ~130 kJ mol^{-1} of internal energy in the radical **18**$^{\bullet}$ formed. The rationale for the extremely large F–C effects is evident from the optimized structures of ion **18**$^{+}$ and radical **18**$^{\bullet}$ (Fig. 14). Ion **18**$^{+}$ has a $T_d \rightarrow D_2$ distorted tetrahedral structure with equivalent P—O bonds. In contrast, radical **18**$^{\bullet}$ is a C_s trigonal pyramid in which the odd electron assumes the fifth axial coordination site on phosphorous. These large differences in the P—O bond lengths and O—P angles account for the substantial F–C effects upon vertical electron capture. The vibrational excitation in vertically formed **18**$^{\bullet}$ exceeds the energy barrier to loss of a hydrogen atom and results in a fast, exothermic dissociation to phosphoric acid. The latter retains most of the vibrational energy, but it is stable enough to resist dissociation. However, the cation radical of phosphoric acid, formed upon subsequent reionization, is much less stable and undergoes facile and almost complete dissociation by loss of OH and elimination of water.[81] The net result is a very weak ion of $H_3PO_4^{+\bullet}$ in the NR spectrum of $P(OH)_4^+$ in spite of the fact that loss of H$^{\bullet}$ is an important dissociation of **18**$^{\bullet}$. Loss of OH$^{\bullet}$ from **18**$^{\bullet}$ gives rise to the stable molecule of trihydroxyphosphane, $P(OH)_3$, which was also character-

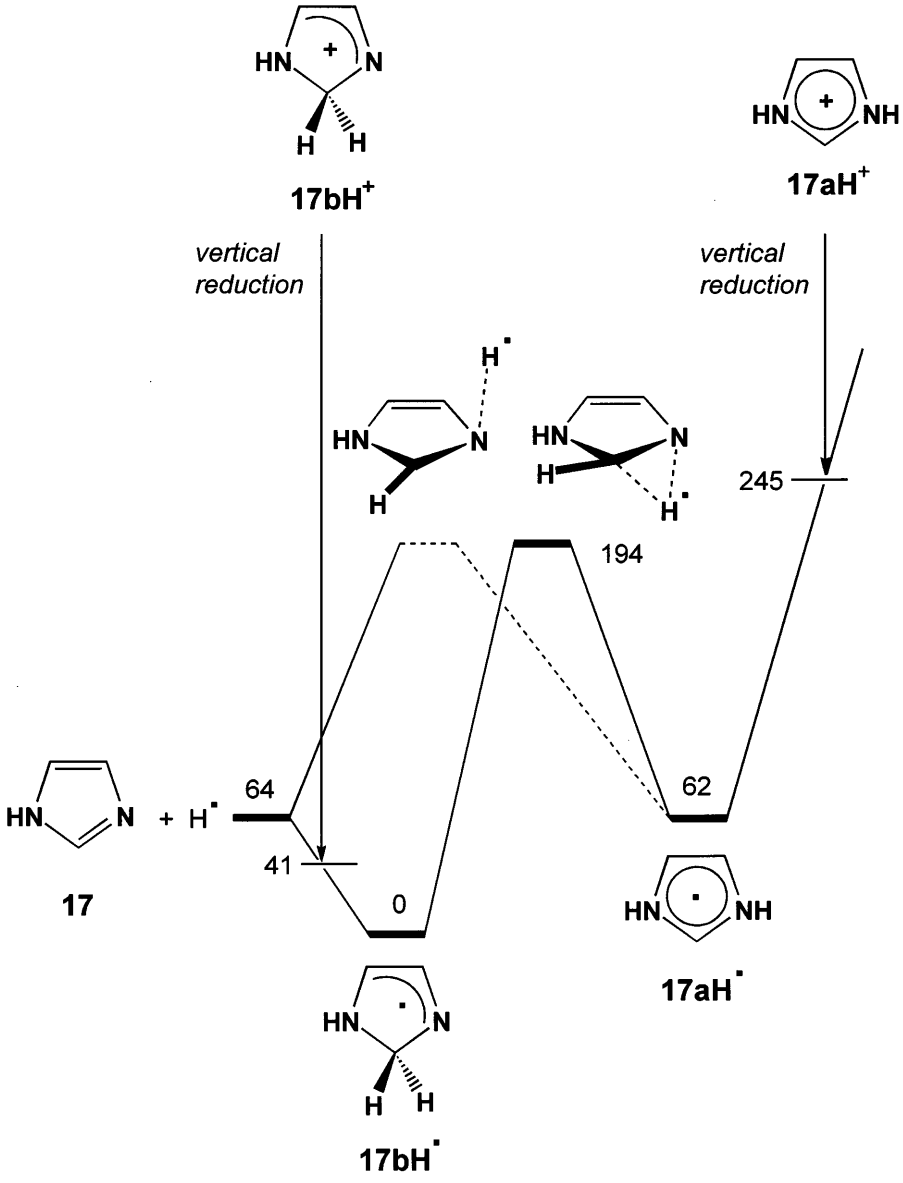

Figure 12. Potential energy profile for neutralization of imidazolium ions **17aH**$^+$, **17bH**$^+$ and dissociations of imidazolium radicals **17aH**$^\cdot$ and **17bH**$^\cdot$.

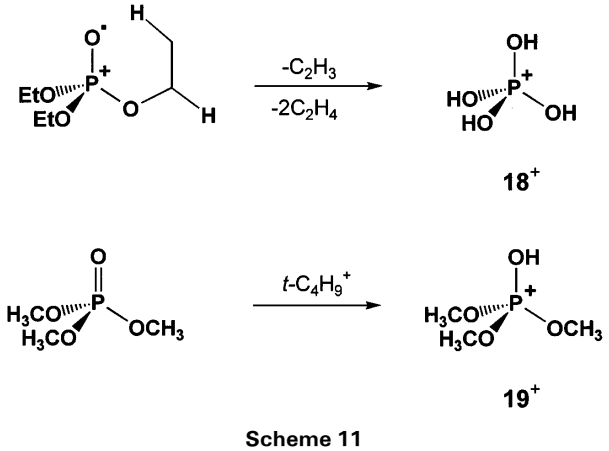

Scheme 11

ized by NRMS and *ab initio* calculations.[81] Radical **18**$^\cdot$ is one of the salient cases of radical systems whose chemistry in NRMS is dominated by F–C effects on vertical electron transfer.[41,43,81]

CONCLUSIONS AND FUTURE OUTLOOK

Mass spectrometric methods based on collisional neutralization of fast ions provide a general strategy for the preparation and study of heterocyclic radicals related to DNA damage. Deuterium labeling, neutral photoexcitation and variable-time measurements are some of the currently available and powerful methodologies to investigate the intrinsic properties of DNA radicals in the gas phase. In addition, the continuing progress in computer technology allows one to address still larger radical systems at unprecedented levels of *ab initio* theory. The symbiosis of experiment and theory lends

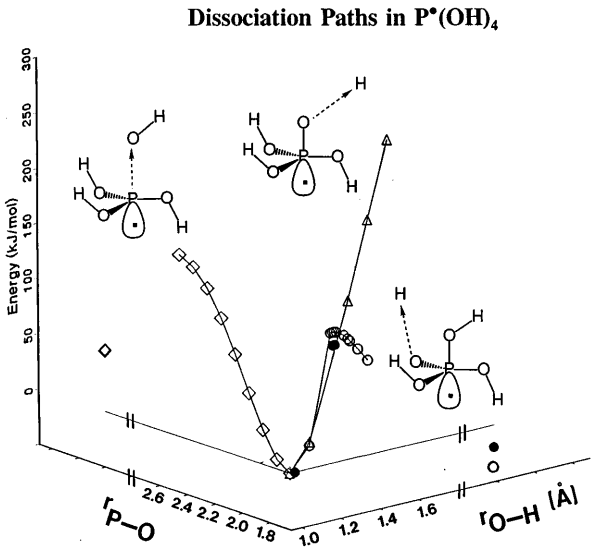

Figure 13. Potential energy profile for dissociations of tetrahydroxyphosporanyl radical **18**•.

the mass spectrometrist an extremely powerful tool to probe these interesting and otherwise inacessible radical systems. It should be noted that preliminary studies of ion–molecule reactions of cation radicals derived from nucleobases have appeared recently,[83] which will further contribute to our knowledge of these fascinating and important species.

Acknowledgements

This work has been supported by grants from the National Science Foundation (CHE-9412774 and CHE-9712570). Computational support by the former Cornell Theory Center, which used to receive funding by NSF, is also gratefully appreciated. Computational support by the computing and Communications Center at the University of Washington and the Computer Cluster in the Department of Chemistry is also acknowledged. The experimental work discussed in this Special Feature was mostly carried out by Dr Viet Q. Nguyen, Ming Gu, and Jill K. Wolken, whose contributions are gratefully acknowledged.

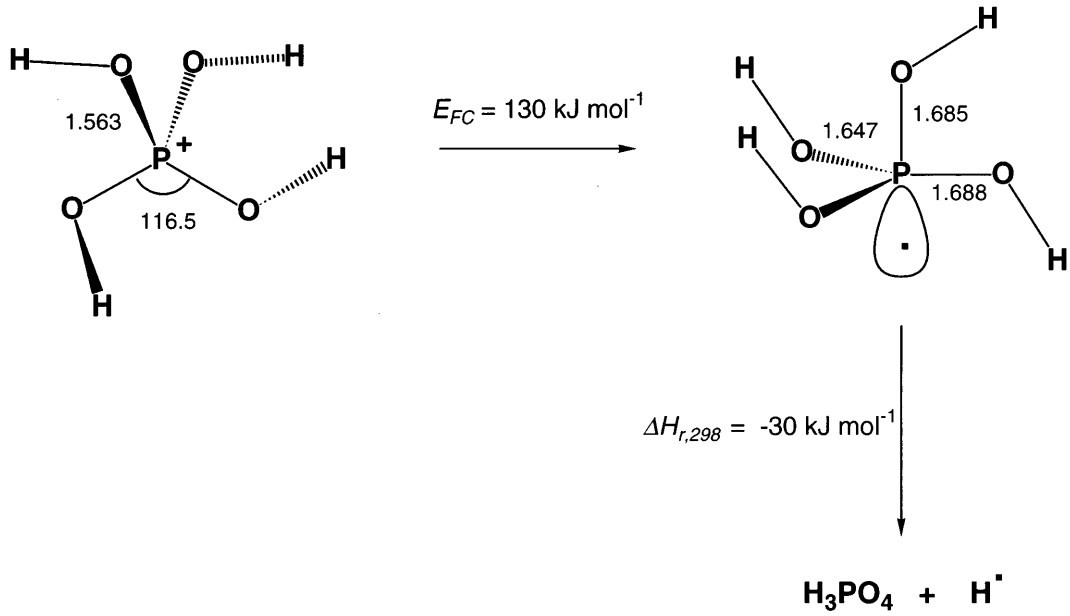

Figure 14. MP2(FULL)/6–31 + G(d) optimized geometries of ion **18**$^+$ and radical **18**•.

REFERENCES

1. W. A. Glass and M. N. Varma (Eds), *Physical and Chemical Mechanisms in Molecular Radiation Biology*. Plenum Press, New York (1991).
2. C. Bernstein and H. Bernstein, *Aging, Sex and DNA Repair*. Academic Press, San Diego (1991).
3. C. Richter, in *Free Radical Toxicology*, edited by K. B. Wallace. Taylor and Francis, Washington, DC (1997).
4. C. von Sonntag, in *Physical and Chemical Mechanism in Molecular Radiation Biology*, edited by W. A. Glass and M. N. Varma, pp. 287–321. Plenum Press, New York (1991).
5. R. Atkinson, *Gas-Phase Tropospheric Chemistry of Organic Compounds, J. Phys. Chem. Ref. Data*, Monograph No. 2, pp. 47–50. American Chemical Society, Woodbury (1994).
6. M. C. R. Symons, *J. Chem. Soc., Faraday Trans. 1* **83**, 1 (1987).
7. W. R. Holley, A. Chatterjee and J. L. Magee, Radiat. Res. **121**, 161 (1990).
8. G. E. Adams and R. L. Wilson, *Trans. Faraday Soc.* **65**, 2981 (1969).
9. K.-D. Asmus, H. Mockel and A. Henglein, *J. Phys. Chem.* **77**, 1218 (1973).
10. P. Neta, *Adv. Phys. Org. Chem.* **12**, 223 (1976).
11. C. von Sonntag, *Radiat. Phys. Chem.* **30**, 313 (1987).
12. S. Steenken, *Chem. Rev.* **89**, 503 (1989).
13. D. M. Close, W. H. Nelson and E. Sagstuen, in *Electronic Magnetic Resonance of the Solid State*, edited by J. A. Weil, p. 237. Canadian Society of Chemistry, Ottawa (1987).
14. J. Geimer, O. Brede and D. Beckert, *Chem. Phys. Lett.* **276**, 411 (1997).
15. M. Dizdaroglu, *Methods Enzymol.* **193**, 842 (1990).

16. D. T. Sawyer, A. Sobkowiak and T. Matsushita, *Acc. Chem. Res.* **29**, 409 (1996).
17. C. Walling, *Acc. Chem. Res.* **31**, 155 (1998).
18. P. A. MacFaul, D. D. M. Wayner and K. U. Ingold, *Acc. Chem. Res.* **31**, 159 (1998).
19. B. W. Williams and R. F. Porter, *J. Chem. Phys.* **73**, 5598 (1980).
20. G. I. Gellene and R. F. Porter, *Acc. Chem. Res.* **16**, 200 (1983).
21. P. O. Danis, C. Wesdemiotis and F. W. McLafferty, *J. Am. Chem. Soc.* **105**, 7454 (1983).
22. P. C. Burgers, J. L. Holmes, A. A. Mommers and J. K. Terlouw, *Chem. Phys. Lett.* **102**, 1 (1983).
23. C. Wesdemiotis and F. W. McLafferty, *Chem. Rev.* **87**, 845 (1987).
24. J. K. Terlouw and H. Schwarz, *Angew. Chem., Int. Ed. Engl.* **26**, 805 (1987).
25. J. L. Holmes, *Mass Spectrum. Rev.* **8**, 513 (1989).
26. J. K. Terlouw, *Adv. Mass Spectrom.* **11**, 984 (1989).
27. F. W. McLafferty, *Science*, **247**, 925 (1990).
28. F. Tureček, *Org. Mass Spectrom.* **27**, 1087 (1992).
29. N. Goldberg and H. Schwarz, *Acc. Chem. Res.* **27**, 347 (1994).
30. C. A. Schalley, G. Hornung, D. Schroder and H. Schwartz, *Chem. Soc. Rev.* **27**, 91 (1998).
31. J. R. Reeher, G. D. Flesch and H. J. Svec. *Int. J. Mass Spectrom. Ion Phys.* **19**, 351 (1976).
32. T. H. Morton, *Tetrahedron* **38**, 3195 (1982).
33. F. P. Lossing, in *Mass Spectrometry*, edited by C. A. McDowell, Chapt. 11, pp. 442–505. McGraw-Hill, New York (1963).
34. F. Tureček, L. Brabec and J. Korvola, *J. Am. Chem. Soc.* **110**, 7984 (1988).
35. D. Griller and F. P. Lossing, *J. Am. Chem. Soc.* **103**, 1586 (1981).
36. J. J. Nash and R. R. Squires, *J. Am. Chem. Soc.* **118**, 11872 (1996).
37. J. C. Poutsma, J. A. Paulino and R. R. Squires, *J. Phys. Chem. A.* **101**, 5327 (1996).
38. A. W. McMahon, S. K. Chowdhury and A. G. Harrison, *Org. Mass Spectrom.* **24**, 620 (1989).
39. G. Hornung, C. A. Schalley, M. Dieterle, D. Schroder and H. Schwarz, *Chem. Eur. J.* **3**, 1866 (1997).
40. L. J. Bellamy, *The Infrared Spectra of Complex Molecules*, Vol. 2. Chapman and Hall, London (1980).
41. C. E. C. A. Hop and J. L. Holmes, *Int. J. Mass Spectrom. Ion Processes* **104**, 213 (1991).
42. F. Tureček, M. Gu and C. E. C. A. Hop, *J. Phys. Chem.* **99**, 2278 (1995).
43. V. Q. Nguyen, S. A. Shaffer, F. Turecĕk and C. E. C. A. Hop, *J. Phys. Chem.* **99**, 15454 (1995).
44. P. O. Danis, R. Feng and F. W. McLafferty, *Anal. Chem.* **58**, 348 (1986).
45. M. J. Polce, S. Beranova, M. J. Nold and C. Wesdemiotis, *J. Mass Spectrom.* **31**, 1073 (1996).
46. D. W. Kuhns and F. Tureček, *Org. Mass Spectrom.* **29**, 463 (1994).
47. D. W. Kuhns, S. A. Shaffer, T. B. Tran and F. Tureček, *J. Phys. Chem.* **98**, 4845 (1994).
48. F. Tureček, M. Gu and S. A. Shaffer, *J. Am. Soc. Mass Spectrom.* **3**, 493 (1992).
49. S. A. Shaffer, F. Tureček and R. L. Cerny, *J. Am. Chem. Soc.* **115**, 12117 (1994).
50. V. Q. Nguyen, M. Sadilek, A. J. Frank, J. G. Ferrier and F. Tureček, *J. Phys. Chem. A* **101**, 3789 (1997).
51. A. J. Frank, M. Sadilek, J. G. Ferrier and F. Tureček, *J. Am. Chem. Soc.* **119**, 12343 (1997).
52. M. Sadilek and F. Tureček, *Chem. Phys. Lett.* **263**, 203 (1996).
53. M. Sadilek and F. Tureček, *J. Phys. Chem.* **100**, 9610 (1996).
54. M. Sadilek and F. Tureček, *J. Phys. Chem.* **100**, 224 (1996).
55. V. Q. Nguyen and F. Tureček, *J. Mass Spectrom.* **32**, 55–63 (1997).
56. C. Hillebrand, M. Klessinger, M. Eckert-Maksic and Z. B. Maksic, *J. Phys. Chem.* **100**, 9698 (1996).
57. W. G. Mallard and P. J. Lindstrom (Eds), *NIST Chemistry Webbook, NIST Standard Reference Database*, No. 69. National Institute of Standards and Technology, Gaithersburg, MD (1998); http://webbook,nist.gov/chemistry.
58. E. Uggerud, *Adv. Mass Spectrom.* **13**, 53 (1995).
59. B. Abel, B. Herzog, H. Hippler and J. Troe, *J. Chem. Phys.* **91**, 900 (1989).
60. H. Hippler and J. Troe, in *Bimolecular Collisions*, edited by M. N. R. Ashfold and J. E. Baggott, Chapt. 5, pp. 209–262. Royal Society of Chemistry, London (1989).
61. R. G. Gilbert, and S. C. Smith, *Theory of Unimolecular and Recombination Reactions*, p. 254. Blackwell, Oxford (1990).
62. V. Q. Nguyen and F. Tureček, *J. Mass Spectrom.* **31**, 843 (1996).
63. V. Q. Nguyen and F. Tureček, *J. Mass Spectrom.* **31**, 1173 (1996).
64. J.-C. Lorquet, B. Leyh-Nihant and F. W. McLafferty, *Int. J. Mass Spectrom. Ion Processes* **100**, 465 (1990)
65. J. K. Wolken and F. Tureček, *J. Am. Chem. Soc.* submitted for publication.
66. A. Les, L. Adamowicz, M. J. Novak and L. Lapinski, *J. Mol. Struct.* (*THEOCHEM*) **277**, 313 (1977).
67. A. R. Katritzky, M. Karelson and P. A. Harris, *Heterocycles*, **32**, 329 (1991).
68. J. S. Kwiatkowski and J. Leszczynski, *J. Mol. Struct.* **376**, 325 (1996).
69. C. Adamo and F. Lelj, *Int. J. Quantum Chem.* **56**, 645 (1995).
70. A. L. Sobolewski, *Chem. Phys. Lett.* **211**, 293 (1993).
71. E. S. Levin and G. N. Rodionova, *Dokl. Chem. Akad. Nauk SSSR* **164**, 910 (1965).
72. P. Beak, *Acc. Chem. Res.* **10**, 186 (1977).
73. G. Bouchoux, J. Y. Salpin and D. Leblanc, *Int. J. Mass Spectrom. Ion Processes* **153**, 37 (1996).
74. J. K. Wolken and F. Tureček, *J. Am. Chem. Soc.*, submitted for publication.
75. V. Q. Nguyen and F. Tureček, *J. Am. Chem. Soc.* **119**, 2280 (1997).
76. F. Tureček, *J. Am. Chem. Soc.*, submitted for publication.
77. A. D. Becke, *J. Chem. Phys.* **98**, 1372, 5648 (1993).
78. P. J. Stephens, F. J. Devlin, C. F. Chablowski and M. J. Frisch, *J. Phys. Chem.* **98**, 11623 (1994).
79. M. Polasek and F. Turĕcek, unpublished results.
80. F. Tureček, *J. Phys. Chem. A.*, **102**, 4703 (1998).
81. F. Tureček, M. Gu and C. E. C. A. Hop, *J. Phys. Chem.* **99**, 2278 (1995).
82. S. M. Gustafson and C. J. Cramer, *J. Phys. Chem.* **99**, 2267 (1995).
83. C. Stumpf and H. I. Kenttamaa, presented at the 46th ASMS Conference on Mass Spectrometry and Allied Topics, Orlando, FL, May 31–June 4, 1998, paper WPA022.